



Model-based experimental analysis of pool boiling heat transfer with controlled wall temperature transients

R. Hohl^a, J. Blum^b, M. Buchholz^a, T. Lüttich^b, H. Auracher^{a,*}, W. Marquardt^b

^a Technische Universität Berlin, Institut für Energietechnik, Marchstrasse 18, 10587 Berlin, Germany

^b RWTH Aachen, Lehrstuhl für Prozesstechnik, Turmstraße 46, 52064 Aachen, Germany

Received 1 October 1999; received in revised form 7 August 2000

Abstract

A model-based approach for design, control, operation, and evaluation of pool boiling experiments with controlled steady-state and transient wall temperature up to 50 K/s is presented. Throughout all phases of the described approach, the requirements on the experimental infrastructure for reproducible boiling experiments are addressed by the integration of theoretical and experimental investigations. In the early design phase, these are concerned with the heater design as well as the development and the optimization of a control concept. Systematic experiments were carried out with the fluorinert FC-72. The liquid boiled on top of a horizontally positioned copper heater with a diameter of 18.2 and 5 mm thickness. Temperature measurements by sheathed thermocouples, implanted inside the heater, are used to obtain transient boiling curves by solving a one-dimensional inverse heat conduction problem (IHCP). At the same wall superheat boiling heat flux increases when transient heating rates are increased. This is the case in all boiling regimes. Transient cooling leads to lower transferred heat fluxes. Very close to the boiling surface, temperature fluctuations as a result of evaporation are measured by six microthermocouples. Analysis of the data shows that there seems to be no distinct difference in the fluctuations with respect to steady-state and transient runs. © 2001 Elsevier Science Ltd. All rights reserved.

1. Introduction

For the design of many technically relevant boiling processes one needs to know the heat transfer for the case of a time-varying mean heating wall temperature. In the following, we will refer to this case as *transient boiling*. We examine *pool boiling* processes here. Some applications of transient pool boiling are water quenching of hot steel rods, emergency cooling of nuclear reactors, or cooling of microelectronic components.

Boiling heat transfer is described by the *boiling curve*, cf. Fig. 1. It describes how the transferred heat flux depends on the wall superheat, i.e., the difference between the heating wall surface temperature and the saturation

temperature of the fluid. Starting at low superheats, the curve passes through the *nucleate* (positive slope), *transition* (negative slope), and the *film boiling* (positive slope) region. We refer the reader to [1] for an extensive review of boiling fundamentals. The characteristic shape of the boiling curve leads to important limitations in the design of technical boiling processes. Close to the local maximum of the boiling curve, the *critical heat flux* (CHF), the required surface area for a given heat flux in heat exchangers and cooling systems is minimal. On exceeding the CHF slightly, however, boiling progresses to a state with level heat flux, but much higher wall superheat in film boiling, since operating points in the transition boiling regime are unstable due to the negative slope of the boiling curve. The resulting wall superheat can lead to the destruction of the heating wall. To avoid such a transition from nucleate to film boiling, the location of CHF must be known with adequate reliability. Although boiling heat transfer has been the subject of intensive research for decades, heat exchanger

* Corresponding author. Tel.: +49-30-314-25710; fax: +49-30-314-21779.

E-mail addresses: auracher@iet.tu-berlin.de (H. Auracher), secretary@lfpt.rwth-aachen.de (W. Marquardt).

Nomenclature		T_W	temperature at the heater surface
K_1	boiling curve slope	T_{sat}	temperature of the saturated fluid
K_C	controller gain	<i>Greek symbols</i>	
\mathbf{p}	parameter vector	α	regularization parameter
s	complex frequency (Laplace domain)	λ	thermal conductivity

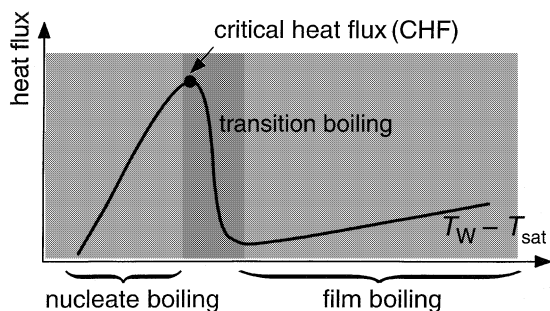


Fig. 1. Typical boiling curve.

design relies entirely, for stationary as well as transient boiling processes, on correlations gathered in stationary boiling experiments [2]. The resulting designs may consequently involve significant uncertainties in the transient case.

There are only a few partially contradicting published studies on transient boiling. Bui and Dhir [3] examined pool boiling of water at atmospheric pressure and found CHF to be lower in cooling experiments than for the heating or the stationary case. Similar results were obtained by Maracy and Winterton [4]. Rajab and Winterton [5] arrived at different conclusions: in their experiments, heating consistently led to lower heat fluxes than at steady-state at the same wall superheat. All three approaches used a similar apparatus, consisting of an electrically heated, vertically or horizontally positioned heating wall. Temperature transients were realized by simply switching the electrical heating on or off, or by step changes in the setpoint of a feedback temperature controller. A different approach was chosen by Peyayopanukul and Westwater [6] who performed liquid nitrogen quenching experiments with test heaters of varying thicknesses and thus varying temperature transients. They found the transferred heat flux to rise with thickness of the heater. However, their presentation of the results does not allow to correlate the momentary heat flux with the gradient of the temperature transient. Also, the transient boiling curves were not compared to curves recorded under stationary conditions. In a recent work of Heas et al. [7], the influence of several heating rates and initial conditions on the boiling incipience is investigated, but only slow transients limited to nucleate

boiling could be realized due to the large thermal inertia of the employed heater.

Unfortunately, all these results are of questionable use. For one, in some studies (such as [5]) no steady-state data for the transition boiling regime could be recorded. Then, only uncontrolled transients, characterized by only one particular temperature transient depending on the thermal mass of the heating wall or the maximum power of the electrical heating, could be realized in any of these experiments. Third, in transient experiments heat flux and temperature at the boiling surface usually have to be estimated from measurements within the heating wall. In [3–6] this is done using simple extrapolation techniques. While these algorithms work well for slow transients and high measurement resolution [8], they are inadequate for the moderate sampling rates achieved in [3–6]; this especially applies to uncontrolled cooling experiments where the boiling state passes very swiftly through the transition boiling region.

In contrast to this, systematic investigations presented in this paper rely on an experimental setup representing technically relevant boiling configurations, in which the important process parameters, i.e., the wall temperature as well as the rate of heating and cooling, can be varied in a controlled fashion. Results for a precursor of the test heater with slow transients and some of the methods used have already been published elsewhere [8–12]. These methods are now applied to implement and evaluate boiling experiments with a new test heater which is optimized for much faster transients. New results will be presented. Fig. 2 shows a schematic sketch of the experimental setup in which the fluorinert FC-72 boils on a horizontally positioned, insulated copper block. At the bottom of the copper block, an electrically powered resistance foil serves as the heat source. For temperature measurements, thermocouples are galvanized into the copper block. In order not to distort the local boiling process, the tips of the thermocouples are located close beneath, but not directly below the boiling surface. The requirements for systematic and reproducible measurements on the experimental infrastructure concentrate on the following three aspects:

- *Homogeneity of the boiling state:* On the one hand, the heater should be as thin as possible to achieve fast transients and favorable control performance, while

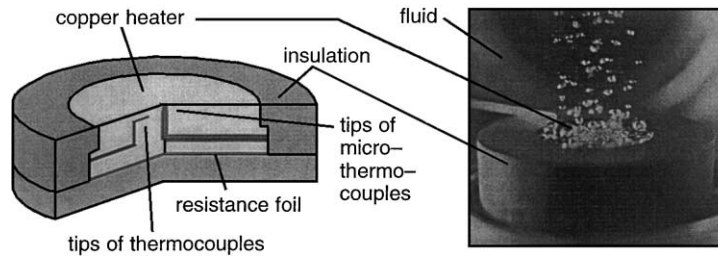


Fig. 2. Principle sketch of boiling experiment.

on the other hand, it should possess enough thermal mass to avoid *heterogeneous boiling states*, which are defined as the simultaneous existence of nucleate, transition, and film boiling on the same boiling surface, implying an overall undefined boiling state. In addition, the homogeneity of the heater's surface, temperature field and the homogeneity of the heat flux through the heater depend on factors such as the geometry of the heater or the choice of insulation.

- **Temperature control:** To enable measurements along the entire boiling curve, operation of the apparatus in transition boiling must be stabilized. This can be achieved passively using stabilizing heating fluids or, as in this study, by means of active feedback temperature control. Beyond mere stabilization, the control concept must allow for the surface temperature to follow a specified reference trajectory in transient experiments.
- **Measurement evaluation:** To infer heat flux and temperature at the boiling surface from heater-interior measurements, a so-called *inverse heat conduction problem* (IHCP) has to be solved. The requirements on a suitable estimation algorithm are computational efficiency and minimization of the estimation problem's high sensitivity to measurement noise.

In the following, these three aspects are addressed using mathematical models of the boiling experiment with a varying degree of detail. A model-based experimental analysis aims at the sound integration of experimental and theoretical investigations. The model-based techniques are here defined in a much broader sense than usually encountered in the boiling literature. As opposed to computer experiments, i.e., mere simulation of more or less detailed boiling models (e.g. in [8]), we use here methods from systems and control theory, signal processing, or numerical optimization as well. Maybe the most important advantage of the chosen approach is that conflicting demands on the design of an experiment can be quantified and brought into accordance. An example which has already been mentioned is the choice of heater thickness, where a large thermal mass of the test heater has opposite effects on the homogeneity of boiling and the controllability of the experiment.

2. Model-based experimental design

2.1. Conceptual test heater design

For fixed heat flux in transition boiling, the negative slope of the boiling curve makes steady-state experiments impossible. Stable operation of the experiment can be achieved in one of the three ways: passive stabilization by means of fluid heating, active stabilization by feedback control adjusting an electrical heating source, or a combination of both approaches. Whether an apparatus can be stabilized depends on a number of factors such as the dimensions and the material of the test heater, the heat transfer characteristics to and from the boiling or the stabilizing fluid, and, in the case of feedback control, the location of the temperature sensors and the employed control law.

By means of a model-based stability analysis and dynamic simulation, the design of a test heater and general parameters for the experimental operation can systematically be optimized *in advance* with respect to stability or control characteristics with dependence on all the above-mentioned parameters even without knowledge of the exact transient boiling heat transfer, but assuming the validity of a steady-state boiling curve.

2.1.1. Detailed finite-element simulations

Detailed three-dimensional finite-element simulations reveal that for the stability analysis and the dynamic simulations for the controller tuning one-dimensional modeling of heat conduction in the copper heater is sufficient. These simulations are carried out employing a three-dimensional finite-element model of the experimental setup including the copper heater and insulation as well as other major components of the heater section using the commercial software package ANSYS.

Deviations from the ideal case of a one-dimensional temperature distribution in the direction perpendicular to the boiling surface can be brought about by heat losses or by discontinuities in the cross-sectional area of the copper block. Fig. 3 shows the simulated temperature field (lines refer to isotherms) of a quarter slice of the heater section at a stationary operating point around

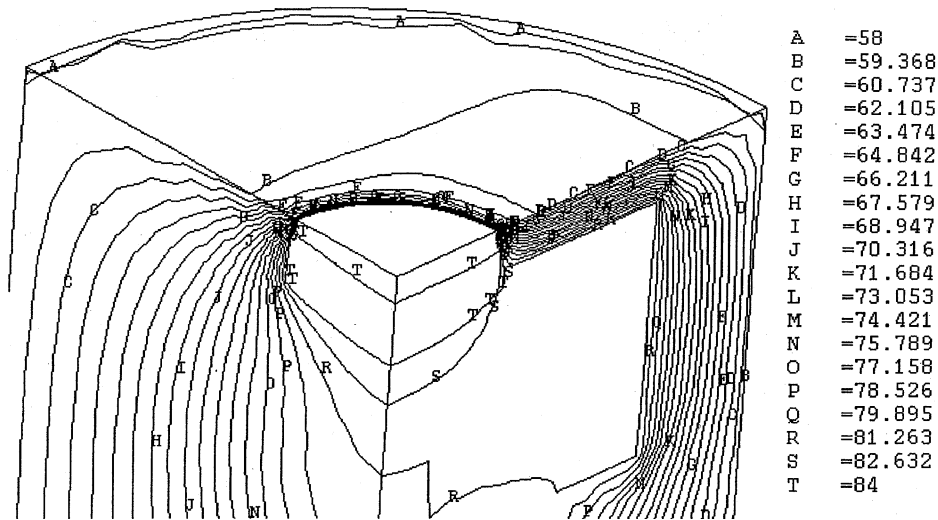


Fig. 3. 3D-FEM-simulation of heater section, isotherms in °C shown.

CHF. Maximum deviation from the average temperature across the surface of the copper heater is found to be less than 0.3 K assuming natural convection at the insulation boundary and boiling at CHF on the heater surface according to experimental data. The results suggest temperature homogeneity at the surface of the heater and a nearly one-dimensional temperature field in the heater.

2.1.2. Stability analysis

The stability analysis which is exactly the same as that of arbitrary linear distributed control systems is based on Laplace domain transfer function models of the test heater, i.e., the heat conduction equation, and all control loop elements such as denoising filters, controllers, or thermocouples. The poles of the closed-loop system are the zeros of its transfer function's denominator, of the so-called characteristic equation

$$g(\mathbf{p}, s) = 0.$$

The roots of the characteristic equation depend on the parameter vector \mathbf{p} , comprising the slope of the boiling curve at the current operating point, the thickness and physical properties of the heater and the controller parameters. The problem of determining the stability limits in a two-dimensional parameter space is equivalent to solving the real and imaginary part of the characteristic equation for two of the variables in \mathbf{p} .

We leave out here the detailed derivation of an optimal stabilization scheme for the heater of Fig. 2 and a comparison of various stabilization methods. These analyses are carried out in [9]. They conclude that feedback control of the heater surface temperature using a proportional-integral (PI-) type controller is the most

flexible approach and suffices for the heater/fluid system considered here.

As an example, Fig. 4 shows the stability limits for a test heater stabilized by PI feedback control in the parameter space spanned by the boiling curve slope K_1 and the controller gain K_C [10]. Both the limits computed from the model and the limits found in experiments are shown. In the face of severe experimental difficulties in obtaining the real stability limits [10], their agreement is excellent. From Fig. 4 it can be deduced which steady-state operating points can be stabilized using a particular controller gain K_C . For $K_1 > 0$ (nucleate or film boiling) the region of stable operation is bounded by only an upper bound. For $K_1 < 0$ (transition boiling) there exists an upper as well as a lower stability bound. The steeper the boiling curve in transition boiling, the smaller the range of admissible controller gains. Operating points beyond a minimal slope cannot be stabilized at all. On the other hand, it is possible to stabilize any operating point along the boiling curve with just one controller gain (here: approx. 5×10^4 W/(m² K)). While Fig. 4 shows the results for a precursor of the test heater presented in this paper, the basic stability characteristics are comparable for both the heaters.

The linear controllability analysis above assumes that there is a uniform boiling state across the surface. It is well known, however, that there are boiling experiments in which nucleate, transition, and film boiling exist simultaneously. This phenomenon of heterogeneous boiling states has often been observed on very thin heaters like wires or foils [13,14].

Our investigations on the stability of heterogeneous boiling states [11,15] for thin and thick heaters are based on a mathematical theory for reaction-diffusion equa-

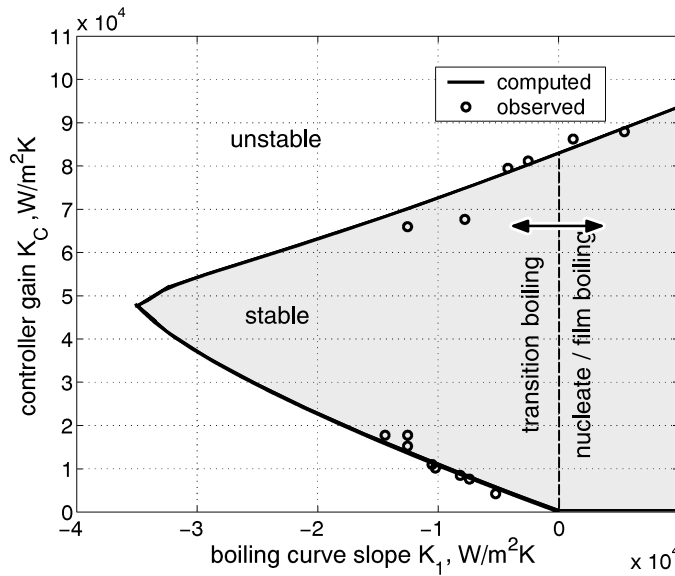


Fig. 4. Experimental validation of theoretically derived stability bounds.

tions [16], which in particular consider the interaction of heat conduction in the heating wall (*diffusion*) and heat removal according to the nonlinear shape of the boiling curve (*reaction*). These reveal that for technically relevant thick heaters as employed in this work, a disturbance, e.g., a spontaneously formed dry spot at the boiling surface impeding heat removal locally, would have to extend up to a few millimeters in order to initiate heterogeneous boiling states. The occurrence of such a large dry spot is highly unlikely. Furthermore, our temperature measurements distributed across the boiling surface indicate a uniform boiling state and a homogeneous temperature distribution in high heat flux nucleate boiling. Thus, these results rule out the possibility of heterogeneous boiling states on the heater employed in this work and contradict the conclusions of Haramura [17] on the existence of heterogeneous boiling states on thicker heaters which we believe, not to be correct [18].

2.1.3. Control performance

There are three aspects which the stability analysis outlined above cannot consider: the effect of the limits of the available heating power and the measurement noise on the achievable control performance as well as the global nonlinearity of the boiling curve. Fig. 5 shows the two principal workings of the feedback controller. The electric power applied to the heating foil is adjusted depending on the difference between the measured temperature and its setpoint value. Steady-state experiments are characterized by stepwise constant temperature setpoints. Once the actual temperature and heat flux settle on the setpoint, data can be recorded. The entire boiling curve is recorded by successively raising or lowering the setpoint value. The main task of control in steady-state experiments can be summarized as stabilizing the transition boiling regime. In transient experiments, the control scheme must additionally ensure a

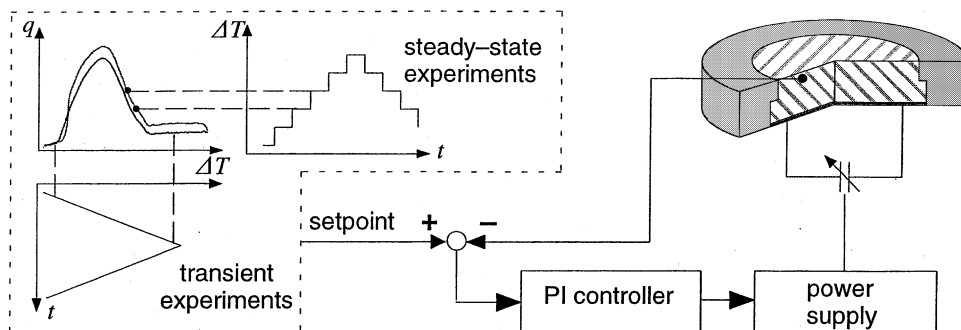


Fig. 5. Control loop.

specifiable temperature trajectory. Here, a ramp with the gradient as the varied parameter and as a measure for transient dynamics is chosen. However, any desired trajectory could in principal be realized.

Once the principal control structure and initial controller tuning parameters have been established by the stability analysis, the parameters are optimized by dynamic simulation of the controlled apparatus. For the PI-controller, which is here augmented by an anti-reset-windup term [19] to minimize the effects of the heating power constraints, the parameters to be optimized are the gain and the reset time. For the gain, a compromise between two concurrent demands has to be found. High gains lead to short controller response times, but high sensitivity to measurement noise. Low gains result in smoother temperature and manipulated variable profiles, but sluggish controller responses and less accurate setpoint tracking. Heater, controller, noise, and setpoint sources are implemented as modeling blocks in the dynamic simulation environment SIMULINK [20]; the boiling curve is approximated by the data from earlier boiling experiments [21].

One goal is to allow the recording of boiling curves with maximal heating or cooling speed. To estimate the achievable limits, the heating case was simulated in SIMULINK by switching on the maximal heating power starting with the apparatus at the saturation temperature of the fluid. The cooling case was simulated by switching off the power supply at a steady-state operating point in film boiling. The results are extreme cases of uncontrolled transients. Since we are interested in heating and cooling processes with a constant slope of the temperature profile, the smallest absolute gradient exhibited in the simulations represents the maximally achievable controlled transients. In simulation, the maximal heating rate was greater than 100 K/s. The fastest realized heating transients were 50 K/s in order to keep a safety margin, whereas the cooling transients

were limited to 4 K/s due to the thermal inertia of the heater.

The simulated controller settling times of about 1 s for steady-state experiments and the tracking errors of the time-varying wall temperature setpoint agree well with those obtained experimentally. Some surface temperature profiles of transient boiling experiments are exemplarily shown in Fig. 6.

The suggested control concept for the first time allows to realize controlled transient experiments. Controlled transients have been attempted previously only in [22]. There, however, only very slow transients (0.2 K/s as opposed to 50 K/s here), which can hardly be classified as truly transient, were achieved; no controlled transients at all were realized in transition boiling. A second advantage of the proposed scheme is the high reproducibility of the results and the high control performance reflected in smooth temperature profiles (see Fig. 6), which is in stark contrast to significant data scattering or missing data from the transition boiling regime representative of many previous studies.

From a control perspective, the relatively large maximum tracking errors of 1.8, 3.8, 11.6 and 23.1 K/s for nominal heating trajectories of 4, 10, 20 and 50 K/s may be considered unsatisfactory. These tracking errors are largely due to thermal inertia of the heater and the fact that the temperature at a thermocouple inside the heater instead of that on the surface of the heater is controlled. Despite these tracking errors, during roughly 90% of the transient time the controller achieves an average wall temperature slope. This slope deviates from the nominal slope by 0.5, 1.7, 5.0, and 8.0 K/s for the nominal heating trajectories of 4, 10, 20 and 50 K/s, respectively. Hence constant and reproducible wall temperature slopes are achieved in all experiments during most of the transients. Another indication of imperfect controller performance is revealed when switching from the heating to the cooling transient,

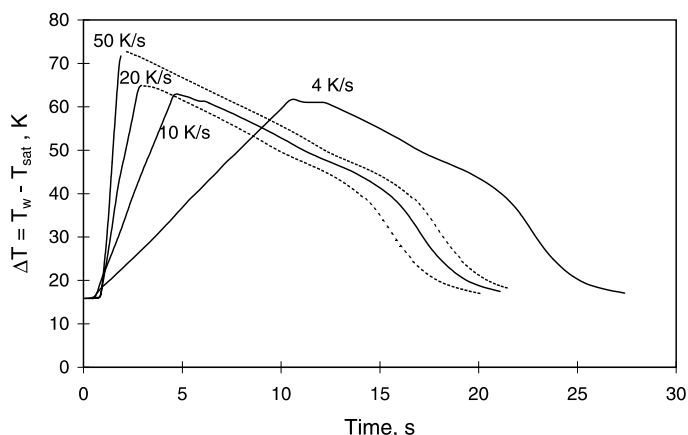


Fig. 6. Measured temperature transients, FC-72, $T_{\text{sat}} = 58^{\circ}\text{C}$.

where – in contrast to the behavior shown in the nominal trajectories of 4 and 10 K/s – a sharp kink occurs. More accurate wall temperature tracking would be indispensable, if a quantitative correlation of the heat transfer coefficient with the wall temperature time derivative should be calculated. At this point, however, we are more interested in the fundamental physical effects of a transient wall temperature on the boiling process. For this purpose, the control performance obtained is fully satisfactory.

Improved control performance would require more advanced control techniques. Instead of feedback control, a two-degree-of-freedom controller could be used to significantly improve tracking performance. In addition to the feedback controller, a feedforward filter could be employed which approximately inverts the transfer function of the heater. In addition, an estimate of the not measurable surface temperature should be used as the control variable for the controller instead of a thermocouple temperature inside the heater wall. This approach would, however, require an on-line solution of the ICHP as discussed below. Tighter control may increase the risk of modifying the nature of the boiling fluctuations by control as discussed in more detail in our previous work [23].

Hence, any improvement in control performance must be carried out with care to make sure that the boiling-induced temperature fluctuations are not modified by control action.

2.2. Experimental facilities

2.2.1. Test apparatus

In Fig. 7, the apparatus with the test heater is shown. The test heater is located at the bottom of a stainless

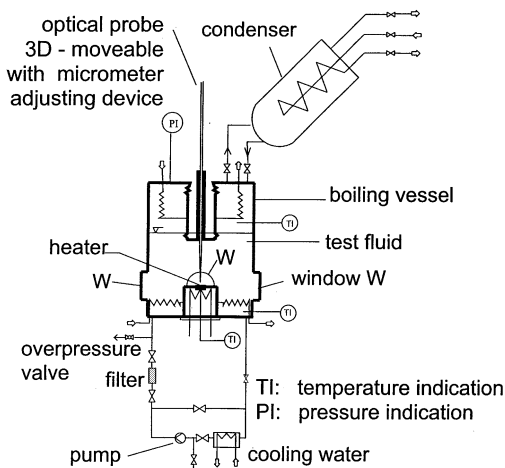


Fig. 7. Test apparatus.

steel vessel (inner diameter: 209.1 mm, height: 332 mm). Four windows enable the observation of the boiling process. The test fluid FC-72 (C_6F_{14} ; 3M-company) is kept at constant saturation temperature by temperature controlled condenser tubes. It can be cleaned from small particles by pumping it through a filter with a mesh size of 40 μ m. Before starting the experiments the test fluid is degassed by boiling in the vessel allowing the noncondensable gases to vent through the condenser. Pressure is measured with a pressure transducer. Liquid and vapor temperatures are measured with four sheathed chromel–alumel thermocouples with 1 mm diameter located at different heights of the vessel. A micrometer adjusting device allows to move an optical probe above the heater surface to study liquid–vapor fluctuations under steady-state conditions.

The test heater, Fig. 8, consists of a 5 mm thick copper block, 20 \times 20 mm squared in the bottom part and cylindrical with 18.2 mm diameter in the top part. It is insulated and sealed by polyimide, a high temperature resistant synthetic, $\lambda = 0.22$ W/(m K). The heating of the copper block takes place by DC flowing through a thin resistance foil (thickness: 0.0125 mm, spec. electrical resistance: 126 $\mu\Omega$ cm). The foil is pressed to the bottom of the heater with a 0.025 mm thick plate of muscovite mica in between for electrical insulation. The maximum possible heating power of the system is 4 kW. Three sheathed Chromel–Alumel thermocouples of 0.25 mm outer diameter are implanted 1.3 mm beneath the heating surface by electroplating. One is used as sensor for temperature control, one as safety sensor against overheating and one to determine the surface temperature. The tips of these thermocouples are located at distances of 5.6, 6.8 and 8.3 mm from the center of the heater.

Chromel–alumel microthermocouples consisting of thin wires with a diameter of 0.025 mm and a 0.002 mm thick polyester coating for electrical insulation were also implanted inside the copper block by electroplating with the top of the thermocouples flush with the top of the copper block. They were located at the center of the heater. The heater surface was covered by a nickel layer of 20 μ m which was ground down to about 10 μ m with E1200 paper. This nickel layer served both for connecting the wires of the microthermocouples and as protection against oxidation of the heater surface. The microthermocouples were small enough that no disturbance of the boiling process could be observed. The results from microthermocouples are quite helpful for a better understanding of the boiling process, but less suitable to determine the shape of the boiling curve. Signals rather reflect the local heat flux than the mean heat flux and exhibit fluctuations as a result of the boiling process. For more details of the experimental facilities see [24].

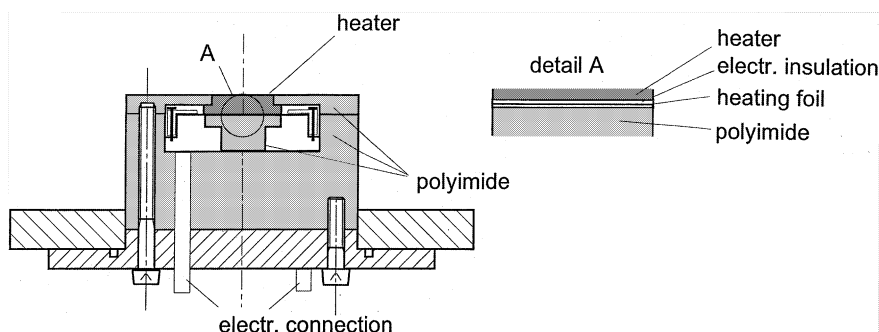


Fig. 8. Test heater.

2.2.2. Control system and data acquisition

The control law, a standard PI-controller with the addition of an anti-reset-windup scheme, was implemented on a signal processing board (AT-DSP2200, National Instruments). The realized time step size of the discrete controller implementation was 1.6 ms. This value is small enough to avoid any difference in controller performance between the continuous-time simulation studies and the discrete-time realization.

Data, i.e., system pressure, heating voltage and amplified temperature signals were sampled with a data acquisition board for PC (PC30, Meilhaus Electronic). The sampling rate for each channel was chosen to be 200 Hz during steady-state experiments, 500 Hz during slow transients up to 15 K/s and 5000 Hz during fast transient runs.

2.3. Measurement evaluation

The thermocouples were calibrated with high precision thermometers with an uncertainty of ± 0.02 K. The uncertainty in temperature measurement, including the uncertainty of both amplifiers and data acquisition board, is ± 0.3 K. To estimate the uncertainty of heat flux additional simulations of the heater including the heating foil and the insulation were carried out. Taking into account uncertainties in voltage measurement, resistance of the heating foil, calculated heat losses at the bottom and side of the heater and of the numerical error of the data evaluation algorithm, the uncertainty of heat flux is less than 20% in nucleate boiling up to CHF, and 30% in transition and film boiling. However, the main aim of this publication is to determine the effect of heating and cooling transients on boiling heat transfer rather than determining boiling curves for the particular experimental setup at high precision. As for all experiments the whole test rig remained unchanged, measurement uncertainties are better represented by the reproducibility of the boiling curves. The variations of heat flux, e.g., at CHF in between experiments with the same temperature transient were less than 6%.

In steady-state experiments data were sampled for 2 s at a frequency of 200 Hz and then averaged for each point of the boiling curve. The heat flux at the heater surface is set equal to the heating power and the surface temperature is calculated by linear extrapolation of the temperature signal 1.3 mm from the surface. In transient experiments both heat flux and temperature at the heater surface are calculated by means of the IHCP algorithm presented next.

2.3.1. The inverse heat conduction problem (IHCP)

For reconstructing the surface heat flux and temperature from heater-interior temperature measurements in transient experiments, a dynamic so-called IHCP has to be solved. IHCPs are ill-posed because of their strong sensitivity to errors such as measurement noise in the input data. Due to the damping effect of heat conduction, temperature changes at the boiling surface are only weakly propagated within the heater. If the measured signal is additionally corrupted by noise, these fluctuations could be misinterpreted as physically meaningful temperature changes at the surface. The quality of a solution algorithm is largely determined by how well two competing objectives can be met at the same time. The two objectives are minimization of the deterministic error assuming error-free measurements on the one hand and suppressing the influence of measurement errors on the estimates on the other. Fast transients call for algorithms much more powerful than previously employed [3–6] for the evaluation of transient boiling experiments.

We have implemented several algorithms, of which a so-called observer algorithm [25] – a filtering approach from systems and control theory – has proven to exhibit the best tradeoff between the mentioned competing estimation objectives. This algorithm is computationally most efficient. It can also be interpreted as a Tikhonov–Arsenin filter [26].

In the past, simple extrapolation techniques have often been used for solving the IHCP [3–6]. For slow transients, these algorithms are principally sufficient.

Even then, however, the quality of the estimation results crucially depends on the parameterization of the solution algorithm. An unfortunate choice of tuning parameters can lead to wrong results. The right choice of the tuning parameter(s) is visualized by the example of Fig. 9 in which a transient boiling curve of 2 K/s is identified from earlier measurements [12] with a different test heater. For too small values of the generic tuning parameter α , which in one form or another is common to all solution approaches, the estimate oscillates around the true curve, indicating quite accurate estimation, but high sensitivity to measurement noise. For large α , the sensitivity and the oscillations vanish, but the dynamics of the estimated boiling curve is significantly damped. The optimal value, indicated by the thick solid line, can be found manually by performing a series of estimation runs. An optimal value is reached if the oscillations in the estimate converge to their moving average. There also exist automated procedures for finding the correct tuning parameters [27,28].

3. Experimental results

All experiments were performed with saturated FC-72 at a fluid temperature of 333 K (saturation pressure 1.3 bar). Before each test run the temperature of the heater was increased until the liquid boiled vigorously. Then the temperature was decreased until only a few activated nucleation sites were present and measurement started. This was done to avoid the effect of delay in boiling incipience. The boiling curve was measured *under steady-state conditions* first at the beginning of all

test runs and second at the end of all test runs to make sure that heater surface conditions did not change during the experiments. For measuring the boiling curve under steady-state conditions, the heater temperature was first increased step by step from nucleate boiling up to film boiling and then decreased, again step by step, until low heat flux nucleate boiling was reached. To make sure that boiling conditions were steady-state, measuring took place after a period in which the heater temperature settled. Boiling curves *under transient conditions* were each measured twice for nominal wall temperature transients of 2, 4, 10, 15, 20, 30, 40 and 50 K/s. Here, starting at a steady-state point in low heat flux nucleate boiling the heater temperature was increased by a constant heating rate until a selected temperature in film boiling was reached, heater setpoint temperature was held constant for 2 s and then decreased to a point in nucleate boiling. Temperature overshoot did occur for fast transients, so only runs with slow temperature transients exhibit a short period between the heating and cooling transient with constant temperature, as can be seen in Fig. 6 for a 4 K/s transient run.

3.1. Steady-state runs

In Fig. 10, the data points of two steady-state runs are plotted, each with increasing and decreasing wall temperature. There is no significant difference between the two boiling curves measured at the beginning and at the end of the test runs, so that obviously the heater surface characteristics did not change during the

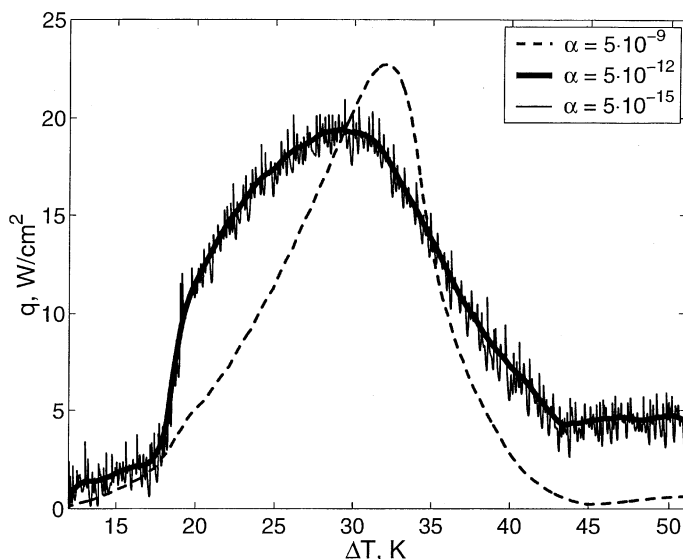


Fig. 9. Estimation of a boiling curve for different settings of the tuning parameter α .

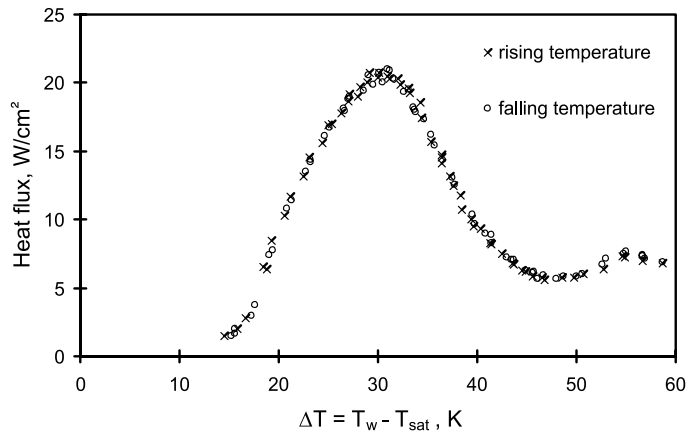


Fig. 10. Steady-state boiling curve, FC-72, $T_{\text{sat}} = 58^\circ\text{C}$.

experiments. Furthermore, the steady-state boiling curve shows no hysteresis for increasing or decreasing wall temperature in the transition boiling region. This confirms earlier results of Auracher [29] and Haramura [30] with R113. It does, however, not agree with Witte and Lienhard's [31] assumption of two transition boiling curves, not with the results measured by Ungar and Eichhorn [32] who measured a hysteresis in their experiments with methanol. The latter suggested that using small heaters with diameters of similar or smaller size than Taylor's most dangerous wavelength [33,34] may explain that no hysteresis occurred in the above-cited experiments. In earlier experiments [35,36] a heater with 34 mm diameter was used, which is more than four times larger than the most dangerous Taylor wavelength (7.9 mm for FC-72 at 60°C). Also in these experiments with FC-72 and a clean heater surface the steady-state boiling curve did not exhibit any hysteresis.

3.2. Transient runs

Boiling curves for transient heating with nominal heating rates of up to 50 K/s are depicted in Fig. 11. For comparison, the data points of a steady-state boiling curve are also plotted.

Since the nominal heating rates given in the legend of Fig. 11 refer to heating rates in the setpoint of the trajectory of the controller, it is to mention that the average heating rates during the transients are 2.2, 4.5, 11.7, 25, 40, 54, and 58 K/s instead of the nominal slopes 2, 4, 10, 20, 30, 40, and 50 K/s, respectively.

The heat flux for transient heating increases with increasing heating rate in all boiling regions. The critical heat flux increases from 20 W/cm² under steady-state conditions to 34 W/cm² for 10 K/s, 55 W/cm² for 20 K/s, to about 85 W/cm² for 50 K/s heating rate. As well as the film boiling heat flux increases considerably from

8 W/cm² under steady-state conditions to more than 50 W/cm² for 50 K/s heating rate.

At a wall superheat of 45–50 K heat flux exhibits a minimum for moderate transients of 15–30 K/s, while it keeps almost a constant value until the end of the heating process during the other test runs. Temperature signals inside the heater do not give any clue to explain this phenomena. However, looking at the boiling process during the experiments, we observed small differences in the macroscopic behavior of the bubbles rising from the heater. During experiments with small heating rates, no difference in bubble rising could be found in comparison to the steady-state behavior. For faster transients of about 20–30 K/s we identified a kind of two clouds of bubbles rising until film boiling was reached which could be the reason for the unusual course of the boiling curve. For faster heating rates, obviously the heating process was so fast, in fact it lasts about 1 s for a 50 K/s transient, that only one cloud of bubbles was observed before a vapor film covered the heater surface.

Due to the thermal inertia of the heater the cooling rates were limited. Constant cooling rates were only possible for 2 K/s along the entire boiling curve and for 4 K/s between transition and nucleate boiling. With uncontrolled cooling, the temperature change was 2 K/s in film boiling and 6.8 K/s at CHF. In Fig. 12, the boiling curves for transient cooling are depicted together with the data points of a steady-state measurement. Obviously, the effect of transient cooling is contrary to the effect of transient heating: the faster the cooling rate the smaller the heat flux. There seems to be a small anomaly in the slope of the boiling curve measured at 4 K/s cooling rate where the boiling curve in transition boiling is shifted to smaller wall superheats. Unlike in the other experiments the heating procedure was stopped already in low heat flux transition boiling to enable a constant cooling rate of 4 K/s. It looks as if not only the wall

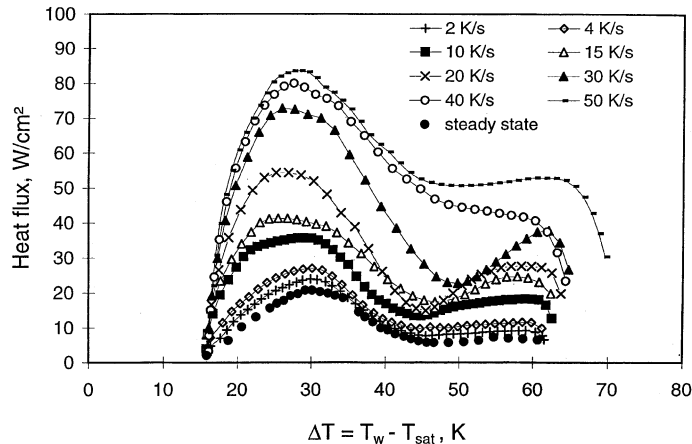


Fig. 11. Boiling curves for transient heating with heating rates up to 50 K/s, FC-72, $T_{\text{sat}} = 58^\circ\text{C}$.

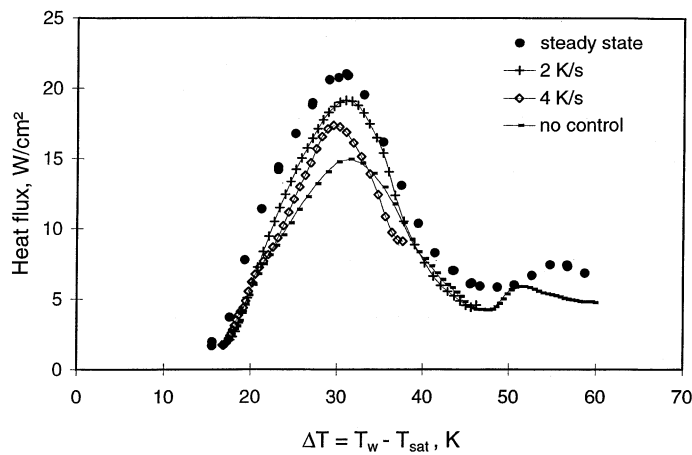


Fig. 12. Boiling curves for transient cooling, FC-72, $T_{\text{sat}} = 58^\circ\text{C}$.

temperature transient has an effect on heat transfer, but the heater temperature at the starting point of the transient cooling process as well. Similar results about the dependence of boiling heat transfer on the initial wall temperature and initial procedures in transient experiments can be found in a recent, more comprehensive study by Heas et al. [7], which is, however, limited to nucleate boiling.

3.3. Interpretation of the experimental results

The results near the critical heat flux and of transition boiling are in qualitative agreement with those of Bui and Dhir [3], Maracy and Winterton [4] and Peyayopanakul and Westwater [6]. However, none of these authors were able to give an explanation for the effect of wall-temperature transients on boiling heat transfer. Rajab and Winterton [5], who opposed the present re-

sults and obtained higher steady-state heat flux than transient heat flux, measured the wetted part of the heater during the experiment. It was dependent on the boiling mode and highest during steady-state experiments where the highest heat flux was obtained.

In film boiling, the heat flux is highly dependent on the temperature transient of the heater surface. Fast temperature increases cause higher heat flux than under steady-state conditions. In cooling mode the effect is vice versa. Measurements with the microthermocouples indicate no wetting of the surface for both steady-state and transient conditions. Further investigations must be done to explain the measured effects in film boiling.

Our results do not give us the information for a straight explanation, but they do give us enough information to discuss what might be a plausible explanation for the influence of wall-temperature transients on boiling heat transfer. If we take a basic look at pool

boiling heat transfer we find three mechanisms: natural convection, vapor formation and convection induced by rising vapor. We can leave out natural convection from further consideration as it is certainly not possible to explain, e.g., the strong increase of heat flux in transient heating along the entire boiling curve with this mechanism. We therefore start by taking a closer look at vapor formation. In earlier experiments, we measured the vapor–liquid fluctuations above the heater by means of an optical probe with a tip diameter of 10 μm , see [35,36]. Unfortunately, it was only possible to use this probe under steady-state conditions. In transient experimentation the distance of the probe tip from the heater surface changed due to the thermal expansion and contraction of both the heater and the probe. The vapor contact times measured at the probe tip at a distance of 0.01 mm from the heater surface were quite short with values up to 10 ms from nucleate boiling up to CHF. In transition boiling the vapor contact times increase until no more liquid contact is detected in film boiling. The increase of the heater temperature in an experiment with 50 K/s heating rate is only 0.5 K during a “long” vapor contact time of 10 ms. So it seems unlikely that the formation of vapor bubbles is influenced by the realized temperature transients in nucleate boiling. An influence in transition boiling is more probable, because here vapor masses stay above the heater surface for a longer time before they rise. In film boiling again the formation of vapor is expected not to be affected by heater temperature transients.

In the test heater, six microthermocouples were implanted (for details see [24]). The measured temperature signals exhibited fluctuations of up to 0.5 K in nucleate boiling and 2 K in transition boiling. The shortest detectable signal rises were in the order of 1 ms. As a result of the manufacturing process the thickness of the nickel layer above the thermocouples is not constant. Therefore the amplitudes of fluctuations were different for each thermocouple. However, comparing these preliminary results of signals of steady-state and transient experiments, no significant differences could be found. Taking the results of both the thermocouples and the optical probe we come to the conclusion that the influence of the present heating and cooling rates on the vapor formation on the heater surface is probably only weak, at least until CHF is reached. It is at least not possible to explain the strong dependence of heat flux on temperature transients.

If neither natural convection nor vapor formation are supposed to explain the strong dependence of heat flux on temperature transients it is necessary to have a closer look at convection induced by rising vapor. In fact we believe that convective heat transfer plays a significant role in the high heat flux region. Nucleating bubbles on the heater surface push the overheated liquid of the macrolayer away and colder liquid from the bulk flows

in. This is especially true for the high heat flux region where Pinto et al. and Gorenflo et al. [37,38] report on nucleation site densities of up to 5.8×10^7 sites/ m^2 . Similar to this mechanism, rising vapor bubbles take along overheated liquid from the vapor liquid interface in film boiling. Under steady-state conditions these steady mixing processes will certainly lead to a less pronounced average temperature gradient from the heater to the bulk as for the transient process. In transient heating the temperature of the liquid flowing from the bulk to the heater surface is colder than under steady-state conditions which leads to higher heat flux. On the other hand, the temperature of the liquid bulk in transient cooling is higher than under steady-state conditions which leads to lower heat flux.

If the above assumption is true, heat flux measured under transient conditions should be dependent on the heater size. The ratio of circumference to surface area is bigger on a smaller heater than on a bigger heater and therefore liquid inflow from the heater side is enhanced. Consequently, a smaller heater is supposed to exhibit a greater dependence on heating rates. This is in fact true. Heat flux for heating transients is significantly higher in the present study than in previous studies with the same experimental and measuring techniques, but a larger heater [35,36]. For cooling transients the result is not so clear because the cooling rates were only small.

If convective heat transfer plays a significant role in high heat flux under transient conditions it does certainly so, to a smaller extent, under steady-state conditions as well. Lienhard and Dhir [34] reported that CHF increased with decreasing heater diameter. They explained this phenomena with Zuber’s theory of thermodynamic instability [33]. Results for CHF measured with FC-72 in [23,29] and the present work exhibit the same trend. It appears to be plausible to explain this behavior with the influence of convective heat transfer.

4. Conclusions

Our model-based experimental analysis, integrating theoretical and experimental efforts, has enabled controlled transient boiling experiments and their reliable evaluation for fast transients up to 50 K/s nominal heating rate and 4 K/s nominal cooling rate.

The boiling curve of FC-72 measured under steady-state conditions exhibits no hysteresis. For transient heating, the heat flux at a given wall superheat along the entire boiling curve increases when the transient heating rates are increased. CHF for 50 K/s heating rate is more than 400% higher than under steady-state conditions. Opposite to this, heat flux for transient cooling decreases with increasing cooling rate. CHF is about 30% lower for uncontrolled cooling with a maximum cooling rate of 6.8 K/s than for the steady-state case. Results from

measurements of liquid–vapor fluctuations above the heater surface with an optical probe and temperature fluctuations on the heater surface with microthermocouples indicate that the influence of convective heat transfer might be the reason for this behavior.

However, more information about the physical processes on the heater surface is necessary to give a definitive explanation for the influence of wall temperature transients on boiling heat transfer. An array of microthermocouples, situated close to each other and very close to the heater surface, will give better information about the local heat flux and the heater surface wetting. So differences in the wetting characteristics, e.g. between transient heating and cooling, could be identified. Additional measurements of liquid–vapor fluctuations above the heater with a number of optical probes can provide results about the size and rising time of vapor masses. Finally, measuring the temperature distribution above the heater with a microthermocouple used as a probe could provide the necessary information to estimate the influence of convective heat transfer in boiling heat transfer.

Acknowledgements

The financial support of the “Deutsche Forschungsgemeinschaft (DFG)” is highly acknowledged. The authors also thank the students who helped with the experimental setup and the data evaluation and 3M Deutschland GmbH for providing us with test fluid FC-72.

References

- [1] V.P. Carey, Liquid–vapor phase-change phenomena: an introduction to the thermophysics of vaporization and condensation processes in heat transfer equipment, in: G.F. Hewitt, C.L. Tien (Eds.), Series in Chemical and Mechanical Engineering, Hemisphere, London, 1992.
- [2] VDI-Waermeatlas (8. Ausgabe), Springer, Berlin, 1997.
- [3] T. Bui, V. Dhir, Transition boiling heat transfer on a vertical surface, *ASME J. Heat Transfer* 107 (1985) 756–763.
- [4] M. Maracy, R. Winterton, Hysteresis and contact angle effects in transition pool boiling of water, *Int. J. Heat Mass Transfer* 31 (1988) 1443–1449.
- [5] I. Rajab, R. Winterton, The two transition boiling curves and solid–liquid contact on a horizontal surface, *Int. J. Heat Fluid Flow* 11 (1990) 149–153.
- [6] W. Peyayopanakul, J. Westwater, Evaluation of the unsteady-state quenching method for determining boiling curves, *Int. J. Heat Mass Transfer* 21 (1978) 1437–1445.
- [7] S. Heas, S. Launay, M. Raynaud, M. Lallemand, Transient nucleate boiling heat transfer from a thick flat sample, in: Proceedings of the Second International Symposium On Two-Phase Flow Modelling and Experimentation, Pisa, Italy, May 1999, pp. 205–210.
- [8] J. Blum, W. Marquardt, Model-based measurement evaluation of transient heat transfer experiments – a comparative study, in: G.P. Celata, P. Di Marco, A. Mariani (Eds.), Proceedings of the Second European Thermal Sciences and 14th UIT National Heat Transfer Conference, Rome, vol. 2, 1996, pp. 1147–1154.
- [9] J. Blum, W. Marquardt, H. Auracher, Stability of boiling systems, *Int. J. Heat Mass Transfer* 39 (14) (1996) 3021–3033.
- [10] J. Blum, W. Marquardt, R. Hohl, H. Auracher, Theory and experimental validation of boiling systems stability, in: Proceedings of the Engineering Foundation Conference Convective Flow and Pool Boiling Paper VII-6, Irsee, 1997.
- [11] J. Blum, Modellgestuetzte experimentelle Analyse des Waermeuebergangs beim transienten Sieden, *VDI Fortschritt-Berichte* 3/557, VDI, Duesseldorf, 1998.
- [12] R. Hohl, H. Auracher, J. Blum, W. Marquardt, Pool boiling heat transfer experiments with controlled wall temperature transients, in: G. Celata, P. Di Marco, A. Mariani (Eds.), Proceedings of the Second European Thermal Sciences and 14th UIT National Heat Transfer Conference, Rome, vol. 3, May 1996, pp. 1647–1652.
- [13] S.A. Zhukov, V.V. Barelko, A.G. Merchanov, Wave processes on heat generating surfaces in pool boiling, *Int. J. Heat Mass Transfer* 24 (1980) 47–55.
- [14] R. Semeria, B. Martinet, Calefaction spots on a heating wall: temperature distribution and resorption, in: Proceedings of the Symposium on Boiling Heat Transfer in Steam-Generating Units and Heat Exchangers, Manchester, England 1965, pp. 192–205.
- [15] J. Blum, T. Luettich, W. Marquardt, Temperature wave propagation as a route from nucleate to film boiling? in: Proceedings of the Second International Symposium on Two-Phase Flow Modelling and Experimentation, Pisa, Italy, May 1999, pp. 137–144.
- [16] P.C. Fife, Mathematical aspects of reacting and diffusing systems, Springer, Berlin, 1979.
- [17] Y. Haramura, Temperature uniformity across the surface in transition boiling, *ASME J. Heat Transfer* 113 (1991) 980–984.
- [18] J. Blum, W. Marquardt, Objection to Haramura’s criteria for temperature uniformity across the surface in transition boiling, LPT-1998-14, www.lfpt.rwth-aachen.de, Lehrstuhl fuer Prozesstechnik, RWTH Aachen, Feb. 1998.
- [19] P. Campo, M. Morari, Robust control of processes subject to saturation nonlinearities, *Comp. Chem. Eng.* 14 (1990) 343–358.
- [20] The MathWorks, Inc., SIMULINK Dynamic system simulation software, 1992.
- [21] J. Blum, R. Hohl, W. Marquardt, H. Auracher, Controlled transient pool boiling experiments – methodology and results, in: D. Gorenflo, D. Kenning, Ch. Marvillet (Eds.), Proceedings of the Eurotherm Seminar No. 48, Pool Boiling, Paderborn, Germany, vol. 2, September 1996, pp. 367–377.
- [22] Y. Haramura, Effect of temperature changing rate and wettability on pseudo-steady transition boiling of saturated water, Proceedings of the Third International Symposium on Heat Transfer, Beijing, 1992.

- [23] H. Auracher, W. Marquardt, The dither-technique for steady-state transition boiling measurements, in: *Proceedings of the Eighth International Heat Transfer Conference*, Hemisphere, New York, vol. 2, 1986, pp. 501–506.
- [24] R. Hohl, Mechanismen des Waermeuebergangs beim stationaeren und transienten Behaeltersieden im gesamten Bereich der Siedekennlinie, VDI Fortschritt-Berichte 3/597, VDI, Duesseldorf, 1999.
- [25] J. Blum, W. Marquardt, An optimal solution to inverse heat conduction problems based on frequency domain interpretation and observers, *Numerical Heat Transfer Part B* 32 (1997) 453–478.
- [26] A.N. Tikhonov, V.Y. Arsenin, *Solutions of ill-posed problems*, V.H. Winston and Sons, Washington, 1977.
- [27] H. Engl, Regularization methods for the stable solution of inverse problems, *Surv. Math. Ind.* 3 (1993) 71–143.
- [28] D. Trujillo, H. Busby, Optimal regularization of the inverse heat-conduction problem, *J. Thermophysics* 4 (1989) 423–427.
- [29] H. Auracher, Transition boiling in natural convection systems, in: *Proceedings of the Engineering Foundation Conference Pool and External Flow Boiling*, ASME, Santa Barbara, USA, 1992, pp. 219–236.
- [30] Y. Haramura, Steady state pool transition boiling heated with condensing steam, in: *Proceedings of the Third ASME/JSME Thermal Engineering Joint Conference*, Reno, USA, 1991, pp. 59–64.
- [31] L. Witte, J.H. Lienhard, On the existence of two ‘transition’ boiling curves, *Int. J. Heat Mass Transfer* 25 (1982) 771–779.
- [32] E.K. Ungar, R. Eichhorn, Transition boiling curves in saturated pool boiling from horizontal cylinders, *ASME J. Heat Transfer* 118 (1996) 654–661.
- [33] N. Zuber, On the stability of boiling heat transfer, *ASME J. Heat Transfer* 80 (1958) 711–720.
- [34] J.H. Lienhard, V.K. Dhir, Hydrodynamic prediction of peak pool-boiling heat fluxes from finite bodies, *ASME J. Heat Transfer* 95 (1973) 152–158.
- [35] R. Hohl, J. Blum, H. Auracher, W. Marquardt, Characteristics of liquid–vapor fluctuations in pool boiling at small distances from the heater, in: *Proceedings of the Eleventh International Heat Transfer Conference*, Kyongju, Korea, vol. 2, 1998, pp. 383–388.
- [36] R. Hohl, H. Auracher, J. Blum, W. Marquardt, Identification of liquid–vapor fluctuations between nucleate and film boiling in natural convection, in: *Proceedings of the Engineering Foundation Conference Convective Flow and Pool Boiling*, Paper II-5, Irsee, Germany, 1997.
- [37] A. Pinto, D. Gorenflo, W. Kuenstler, Heat transfer and bubble formation with pool boiling of propane at a horizontal copper tube, in: *Proceedings of the Second European Thermal Sciences Conference*, Rome, ETS Pisa, Italy, vol. 3, 1996, pp. 1653–1660.
- [38] D. Gorenflo, A. Luke, E. Danger, Interactions between heat transfer and bubble formation in nucleate boiling, in: *Proceedings of the 11th International Heat Transfer Conference*, Kyongju, Korea, vol. 1, 1998, pp. 149–174.